

# Investigation on Ship Collision Phenomena by Analytical and Finite Element Methods

Abuzar.Abazari, Saeed. Ziaei-Rad, Hosein. Dalayeli

**Abstract**—Collision is considered as a time-depended nonlinear dynamic phenomenon. The majority of researchers have focused on deriving the resultant damage of the ship collisions via analytical, experimental, and finite element methods. In this paper, first, the force-penetration curve of a head collision on a container ship with rigid barrier based on Yang and Pedersen's methods for internal mechanic section is studied. Next, the obtained results from different analytical methods are compared with each others. Then, through a simulation of the container ship collision in Ansys Ls-Dyna, results from finite element approach are compared with analytical methods and the source of errors is discussed. Finally, the effects of parameters such as velocity, and angle of collision on the force-penetration curve are investigated.

**Keywords**—Ship collision, Force-penetration curve, Damage

## I. INTRODUCTION

IN the present study, the key focus is on the simulation of the structural strength of ships during the collision by analytical and finite element methods. It is noteworthy that the derivation of the collision damage in huge body like ships using experimental methods is not economical. This has been the main rationale behind the development of analytical and finite element methods in recent years. Therefore, the use of these techniques for simulating ship collision phenomenon is of adequate justification. Yang and Pedersen are among the first researchers who developed analytical methods to model the collision of a container ship. Due to the simplicity of the governing equations in analytical methods, their results may show significant differences when compared with real data also with those obtained from explicit finite element models. This paper uses Ansys/Ls-Dyna to simulate the finite element model. Originally, an exact modeling of the bow and creation of the beams in aft of the bow is constructed to apply mass and moment of inertia of the ship to that. Although, the modeling is accomplished exactly, but due to the nature of the solution in finite element model, there may exist some differences between FE results and the real test data. Therefore, some of these errors are distinguished and the model is revised accordingly. Finally, the verified model is used to illustrate the effects of some of the parameters such as collision angle, friction, and strain rate on the force-penetration curve.

Abuzar, Abazari Faculty of Marine Engineering, Chabahar Maritime University, Chabahar, Iran (phone: 0098-545-412-2181; fax: 0098-545-222-4265 ; email: abazari@cmu.ac.ir).

Saeed. Ziaei-Rad, Department of Mechanical Engineering, Isfahan University of Technology, Isfahan, Iran (e-mail: szrad@cc.iut.ac.ir). (e-mail: author@lamar.colostate.edu).

Hoseyn. Dalayeli, Department of Mechanical Engineering, Malek Ashtar University of Technology, Isfahan, Iran, (e-mail: dalayeli@yahoo.com).

## II. LITERATURE REVIEW

In internal mechanic, to determine the damages in ship collisions, attempts are classified into the following four categories:

*1-Empirical relations 2-Finite element methods 3-Experimental methods 4- Simplified analytical relations.*

For the first category, Minorsky [1] was the first who studied head on collision of a nuclear ship in 1959. He concluded that the relation between the absorbed energy and dissipated volume is linear in high energy collisions. Other researchers such as Jone and Mcdermott [2], Reardon and Sprung [3], Vaughan [4], Voisin [5], and Paik [6] denoted formulas for low energy collisions.

For the second category, Sano and Muragish (1996) [7], Kuroiwa (1996) [8], Kitamura (1997) [9] are among the researchers who investigated the ship side collisions. Amdahl and Kavlie (1992) [10], Lemmen and Vredeveldt (1996) [11] investigated grounding collision of the ship while Lemmen and Yu [12] did some pieces of research in bow crashing.

For the third category, in some of the countries such as Italy, Japan, Germany, and Netherland many experiments on ship collisions have been carried out since the early 1960. The main purpose has been to design nuclear powered ships and protect their nuclear reactors from the menace of collision damages.

In Italy, more than 24 experiments on ship models were conducted to examine the efficiency of different types of side structures towards various types of striking ships. In Germany tests on 12 ship models were carried out. In their experiment, a striking bow running down from an inclined railway path created the collision damage. In Japan, a series of collision model tests was conducted to study some parameters such as the design of side structure, the effect of the shape of striking bow. Amdahl and Kavlie [10] (1992) performed model tests simulating on a double hull indented. Full-scale dynamic collision tests were also carried out by Qvist et al [13]. (1995).

Simplified methods are based on the upper-bound theorem and some assumptions from observations of accidental damages and experimental studies. A major assumption in the simplified analytical methods is that different structural members, such as side shell, decks and frames, do not interact but contribute independently to the total collision resistance.

McDemott et al (1974) [14], Reckling (1983) [15], Amdahl (1983) [16], Yang and Caldwell (1988) [17], Kierkegaard (1993) [18], Hysing (1995) [19], Scharre (1996) [20] and Wang and Ohtsubo (1997) [21] are those who developed and presented a series of simple formulas for ship collision.

In this paper, first, some analytical methods for ship collisions are briefly explained. Next, a case study is considered and the results from different methods are

compared. Then, a finite element model of the ship is constructed and run with Ansys/Ls-Dyna. Finally, the results from FE model are compared with the analytical and empirical formulas.

### III. THEORY

Amdahl's method has been established on the basis of theoretical considerations[22]. It considers the dissipated energy during plastic deformation of the basic structural elements such as angles, T- and cruciform sections. The total crushing load of a specific structure is then determined by adding up all contributions of the basic elements that comprise the actual cross-section. For each element, the folding length and crushing load is determined by a minimization of the absorbed deformation energy during the folding process.

The crushing model that proposed by Yang and Caldwell, to a large extent, is based on the same deformation and energy evaluation as made by Amdahl. Yang and Caldwell assume somewhat different energy dissipation during deformation of the considered structure. In addition, Amdahl showed that via a minimization of the deformation energy absorbed during the folding process the folding length and crushing load can be determined where Yang and Caldwell proposed that the folding length  $H$  is equal to the spacing between transverse frames, provided that the frame spacing is less than the theoretical folding length.

Pedersen [23] applied previous methods to low scale bow and compared their results together also with those obtained from the experimental results. He also suggested a simple formula for estimation of the collision force and force-penetration curve. This formula takes into the account the effects of the strain rate, collision velocity, and ship size.

The added mass is an important parameter that is defined when an object moves in fluid. The acceleration of the fluid is due to the body motion and hydrodynamic effects. For simplicity in equations, the virtual mass is added to the actual mass. This virtual mass depends on the geometry of the object. In table 1 the value of penetration and time of collision based on Pedersen's empirical-analytical method, also the maximum force by which a bow damages based on Saul-Sevensen formula are shown.

### IV. CASE STUDY

Container ships are gigantic ships which are usually used for transportation purposes. The issue of traffic in ship routing has greatly increased the risk of ship collision in nowadays transportations. One of the critical collision conditions is called head-on collision which is investigated in more details in this section. In table I the characteristics and dimensions of the ship [25]. and its bow have been illustrated.

TABLE I

DIMENSION AND CHARACTERISTIC OF A 40,000 DWT CONTAINER SHIP	
length between perpendiculars:	<b>211.50 m</b>
breadth moulded:	<b>32.20 m</b>
depth moulded:	<b>21.00 m</b>
depth to forecastle deck:	<b>24.00 m</b>
Max. draft:	<b>11.90 m</b>
displacement loaded:	<b>54,000 tonnes</b>
Max. service speed:	<b>11.3 m/s</b>
The bulbous bow is stiffened longitudinally. The transverse frames supporting the Longitudinals have a spacing of 2.4 m. The structural data for the bow are as follows.	
Material:	
yield stress for plates and stiffeners (at):	<b>235.0 MPa</b>
ratio between ultimate- and yield stress ( $\sigma_u/\sigma_y$ ):	<b>1.9</b>
Bottom:	
plate thickness:	<b>19.0 mm</b>
longitudinals, spacing 0.8 m:	<b>L250 x 90 x12/16</b>
<i>CL-girder</i> :	<b>L1900 x 250 x 15/25.</b>
Side shell:	
plate thickness, side shell up to 6.1 m abl:	<b>17.0 mm</b>
plate thickness, side shell between 6.1 and 12.3 m abl:	<b>35.0 mm</b>
plate thickness, side shell between 12.3 and 21.0 m abl:	<b>16.0 mm</b>
plate thickness, side shell above 21.0 m abl:	<b>14.0 mm</b>
longitudinals below 5.2 m abl and above 13.6 m abl, spacing 0.8 m:	<b>L250 x 90 x 10/15</b>
Longitudinals between 6.6 and 12.0 m abl, spacing 0.6 m:	<b>L250 x 90 x 12/16.</b>
Forecastle deck, 24.0 m abl:	
plate thickness:	<b>15.0 mm</b>
longitudinals, spacing 0.8 m:	<b>L150 x 100 x 9</b>
<i>CL-girder</i> :	<b>L700 x 150 x 12/12.</b>
Main deck, 21.0 m abl:	
plate thickness:	<b>11.0 mm</b>
longitudinals, spacing 0.8 m:	<b>L150x 100 x 9</b>
<i>CL-girder</i> :	<b>L700 x 150 x 12/12.</b>
Deck, 17.6 m abl:	
plate thickness:	<b>I 1.0 mm</b>
longitudinals, spacing 0.8 m:	<b>L150x 100x9</b>
<i>CL-girder</i> :	<b>L700 x 150 x 12/12.</b>
Deck, 12.8 m abl:	
plate thickness:	<b>15.0 mm</b>
longitudinals, spacing 0.8 m:	<b>L200 x 90 x 9/14</b>
<i>CL-girder</i> :	<b>L700 x 150 x 12/12.</b>
Deck, 6.0 m abl (not W.T.):	
plate thickness:	<b>11.0 mm</b>
Longitudinals, spacing 0.8 m:	<b>Fl.150 x 12.</b>

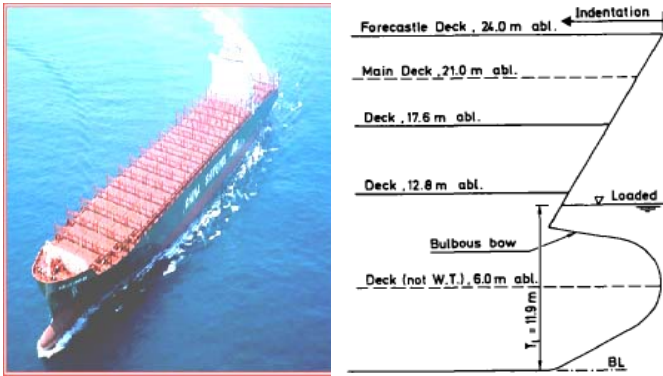


Fig. 1 Dimensions of container ship bow(left)- a picture of the container ship (right)

V. RESULTS FROM ANALYTICAL METHODS

Due to the large amount of calculations required for Yang’s method, this method is programmed in a Fortran environment. After running the developed program for 12 sections of the bow, the force-penetration curve of a head-on collision obtains that is depicted in Fig. 2. Note that the effect of strain rate has not been considered in this figure. The force-penetration curves of this special container ship has been derived from Pedersen’s article [23]. and are mainly based on the methods developed by Yang, Caldwell, and Amdahl. The curves are shown in Fig. 1. The data are recalculated for two different strain rates (i.e. constant and variable strain rates) and the results are compared with those reported by Pedersen in Fig. 3.

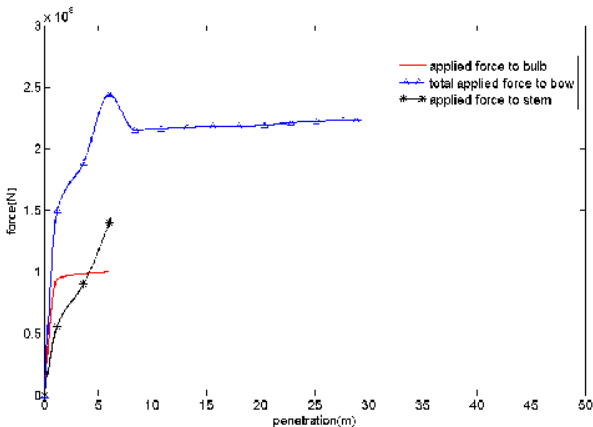


Fig. 2 derived Force-penetration curves from analytical yang method (neglecting the effect of strain rate)

Initial velocity for all of curves is considered to be 12.9 m/s. The effect of strain rate is applied using several formulas. Gerard’s formula is used to determine the strain rate. To relate the static stresses to the dynamic ones, a number of other formulas including Gerard [26]., Cowper Symon, and Manjoine [27]. are used. In the present study, strain rate is assumed to be varied by the use of linear velocity reduction assumption. In most studies, it is assumed that the total kinetic energy is dissipated due to the plastic deformation, and friction is neglected. It should be pointed out that the effect of friction in head-on collisions is low in practice. As shown in

Figure 3, since Manjoine and Gerard’s formulas use dynamic effective stress that is the average of the yield and ultimate stresses, they result in similar curves.

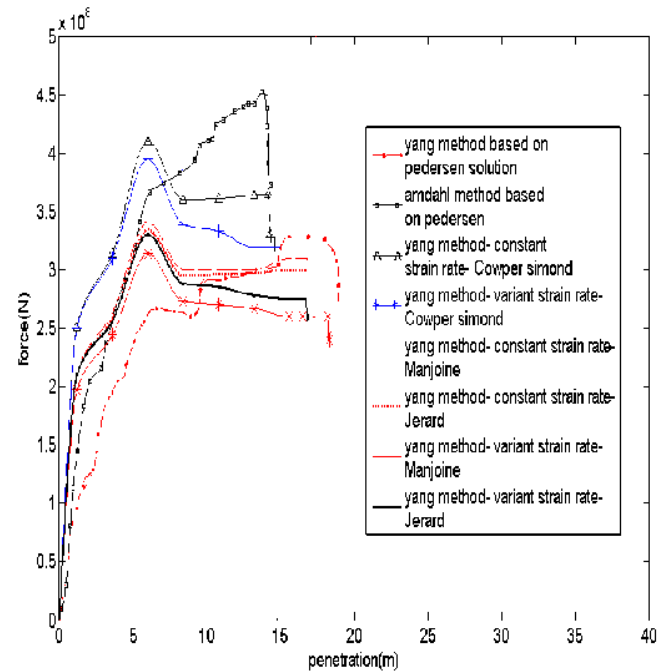


Fig. 3 Comparison of force-penetration curves for Yang and Pedersen results [23] based on Yang and Amdahl’s methods - the initial velocity of the ship is 12.9 m/s .

Figure 4 plots the results from a comparative study between force-penetration curves of different velocities 3, 6, 11.3, 12.9, and 17.52 m/s. The curves in Figure 4 are without strain rate effect. In Fig. 5 by applying the strain rate, a comparison is made between Pedersen and Yang’s methods. The results confirm that the calculated penetration values from Pedersen’s method are less accurate in comparison with the results evaluated from Yang’s method. The results indicate that as velocity increases, this difference goes higher and becomes more significant

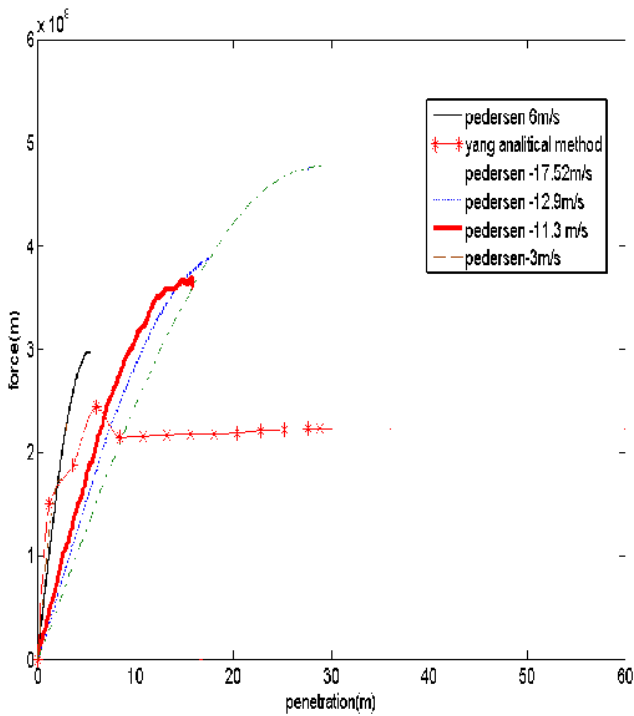


Fig. 4 Force-penetration curves based on Pedersen's method for different velocities

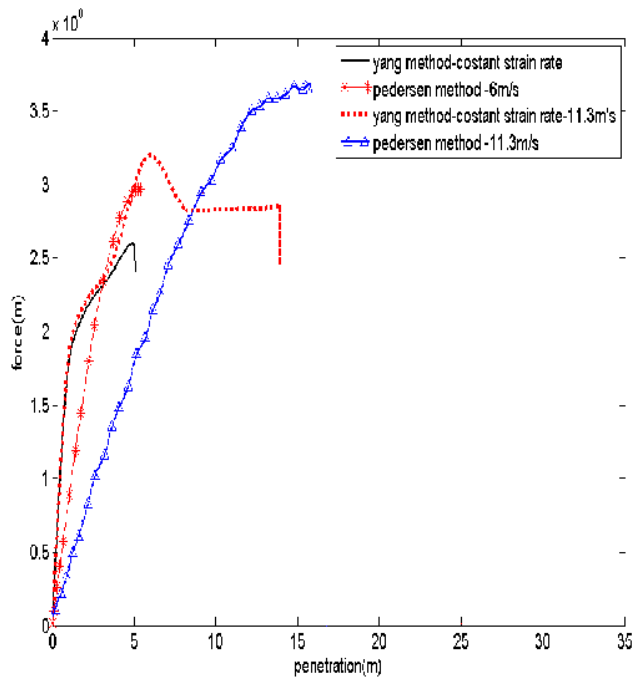


Fig. 5 Force-penetration curves for velocity=6, 11/3 m/s based on Pedersen and Yang's methods (with effect of strain rate)

The value of penetration and time of collision by Pedersen's empirical-analytical method and also the maximum force for damage bow based on Saul-Sevensen's formula [28] are shown in Table II.

TABLE II  
PENETRATION AND MAXIMUM FORCE AND TIME COLLISION FOR DIFFERENT VELOCITIES

Velocity $m/s$	Pedersen method		saul-sevensen		US GUIDE
	Time of collision $S$	maximum penetration $m$	maximum collision load $MN$		
3	1.3	2.3	174	176	72
6	1.5	5.4	297	176	144
11.3	2.3	15.5	367	176	271.2
12.9	2.5	19	392	176	309.6
17.5	2.7	28.8	474	176	420.5

Up to this point, comparisons between the obtained results from different analytical methods have been illustrated. In the next section the ship collision is modeled through Ansys-Ls-Dyna.

### VI. MODELING OF SHIP COLLISION BY ANSYS-LS-DYNA

#### A. Applying added mass to the ship model

In the developed finite element model, the bow is modeled completely. However, for the aft of the bow instead of modeling all elements of the ship, some longitudinal beams with special densities are used to provide the equivalent mass and moment of inertia of the whole ship correctly (Figs. 6,7,8).

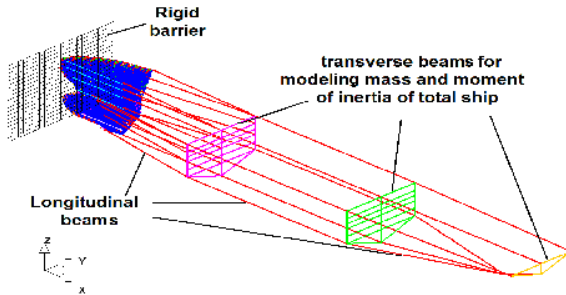


Fig. 6 General view of ship container model

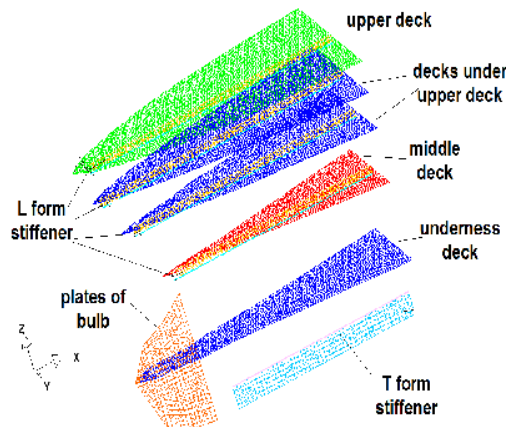


Fig. 7 General view of decks and girder of bow

For simplicity in modeling, the stiffeners which are located on bow decks are replaced with some extra thickness in plates similar to what has been carried out by Xia [25].

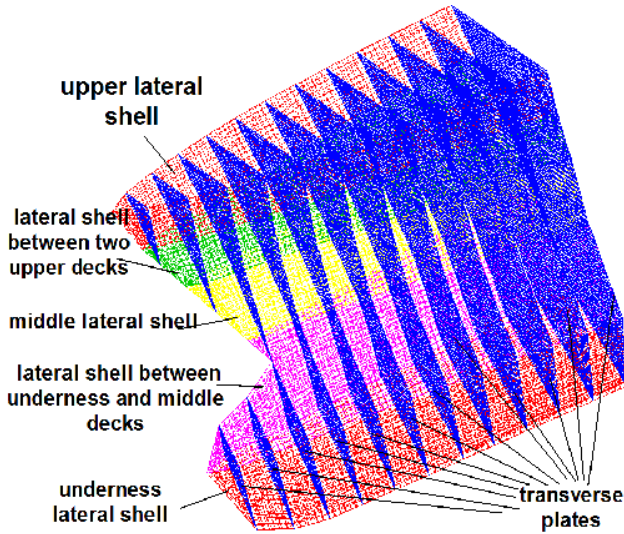


Fig. 8 General view of shells and transverse plates of bow

For applying added mass to the ship, first, the following data are needed to be considered:

Bow mass	$203.1 \times 7.85 \times 10^3 = 1.59 \times 10^6 \text{ Kg}$
Added mass in surge direction	$54 \times 10^6 \times 0.05 = 2.7 \times 10^6 \text{ kg}$
Virtual mass in surge direction	$54 \times 10^6 + 2.7 \times 10^6 = 56.7 \times 10^6 \text{ kg}$
Actual moment of inertia in yaw direction	$(55.78)^2 \times 54 \times 10^6 = 1.68 \times 10^{11} \text{ kgm}^2$
Virtual moment of inertia in yaw direction with coefficient (.021)	$1.68 \times 10^{11} \times 1.21 = 2.033 \times 10^{11} \text{ kgm}^2$
moment of inertia of bow about mass center of ship	$1.59 \times 10^6 \times (60)^2 = 5.724 \times 10^9 \text{ kgm}^2$

The defined added mass coefficients in the above section are calculated based on reference [24] which are:  $C_{11} = 0.05$ ,  $C_{22} = 0.85$ ,  $C_{33} = 0.21$ .

After calculating the added mass in surge and yaw directions for the container ship by applying two equations, the beam density in aft of the bow is derived by the following two relations:

- Mass of longitudinal beams + mass of transverse beams + mass of bow = total virtual mass  
Yaw moment of longitudinal beams + Yaw moment of transverse beams + Yaw moment of bow = total virtual Yaw moment

Finally, the density of each section is derived as:

$$\rho_1 = 30406.3 \text{ kg/m}^3, \rho_2 = 9709.63 \text{ kg/m}^3$$

### B. Material properties

Two types of material are used for the modeling, rigid for barrier and elastic-plastic model for any element of the ship. The Characteristic of all parts of the model are shown in Table III.

TABLE III  
CHARACTERISTIC AND MATERIAL PROPERTIES USED IN CONTAINER SHIP MODELING

Barrier	Longitudinal beam in aft of bow	bow	Transverse beam in aft of bow	Part
rigid	elastic-plastic	elastic-plastic	elastic-plastic	Material model
$7.85 \times 10^3$	30574.78	$7.85 \times 10^3$	6686183	density
2.09E11	2.09E11	2.09E11	2.09E11	Elasticity module
0.28	0.28	0.28	0.28	Poisson coefficient
1	3.4E8	3.4E8	3.4E8	Yield stress
7	40	40	40	C-strain rate parameter
7	5	5	5	P- strain rate parameter

### C. Contact and boundary conditions

Belytschko-Tsay and Hughes- Liu elements are used, respectively, to mesh shells and to model the beams.

A node to surface contact model was used for the contact between different part of the ship with the rigid part and also with each others. The friction coefficients which were used for this model are similar to those reported by Brown [24].

Initial velocity is applied to all nodes of the ship. The boundary conditions are assumed to be as follows: all nodes of the barrier are constrained in all directions and nodes which are located on the collision bulkhead are constrained in translation z and x, y rotation by Xia's technique [25].

It should be noted that because of the lack of uniform mass distribution, if movement constraint in the z direction is not applied on the collision bulkhead nodes, a nose down phenomena is created as stated in Jianjun's thesis [25]. This means that because of modeling the aft of the ship by beams, distribution of the mass in direction z may not be uniform. In order not to have the nose down while the ship is colliding, that doesn't happen in reality, displacement of direction z should be restricted.

## VII. COMPARISON OF FINITE ELEMENT AND ANALYTICAL RESULTS

### A. Force-penetration curve

There are some maximum and minimum points on the force-penetration curve from finite element model. Unlike the FE results, the analytical curves are smooth and do not contain any sharp point and changes. This is because of plastic hinge line forming on plates that reaches yield stress. These plates are located between bow transverse plates. Explanation of this fact is as follows: when a transverse frame contacts with rigid barrier, the plates that is located between this transverse plates and next frames such as L, T, cruciform (decks, lateral plates, girder etc) bear uniform force. When collision occurred, the stresses in plates increase until the whole section is reached to its ultimate stress. In this moment, plastic hinge line is formed and collapse mechanism is occurred. After this time no resistance is bear by these plats. Value reduction on force-penetration curve, after the peak, continue until next

transverse frame contact with rigid barrier and curve gradient will be positive again.

*B. Finite element versus Yang analytical results*

It is important to compare two curves with the same conditions such as, loading, material, velocity, etc. The maximum values of the curve happen at the following points: At the instance that the total section reaches the yield stress and in the instance right before the collapse occurs. Therefore, it is acceptable to compare the Yang's analytical method with a curve that connects the maximum points of the finite element curve as shown in Fig. 9.

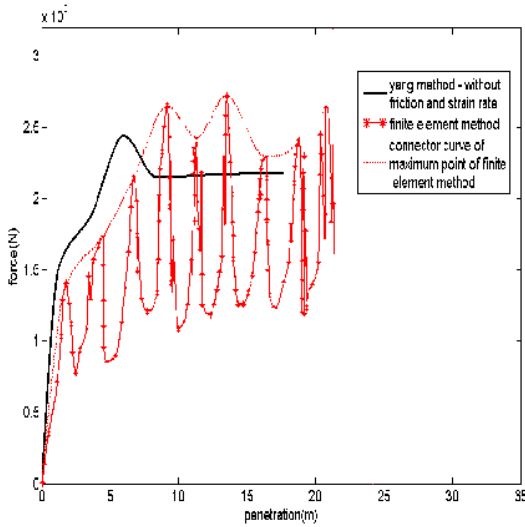


Fig. 9 Comparison of the force-penetration curves obtained from Yang's method and the finite element method

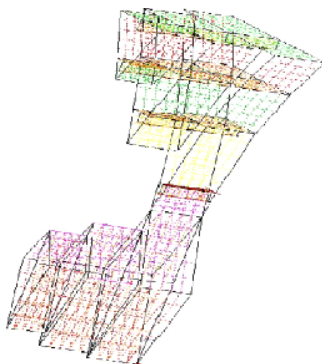


Fig. 10 Considered sections in analytical Yang's method

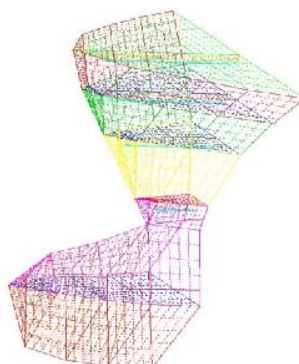


Fig. 11 Actual form of bow Finite Element

Difference in results may divide into two parts: 1- before the fourth section 2-after the fourth section.

In the first three sections, values calculated by finite element are less than those by analytical method. This is reasonable because the analytical relations by which the collapse force is derived are based on the assumption that the section forms uniformly (Figure 10) while the finite element model analyzes the real form of bow (Figure 11).

After the first three sections, the forces predicted by finite element method are less than those obtained from the analytical method. In spite of having similar shapes for sections in both methods, analytical method assumes that constrains on the edges of the structural elements are simply supported while all the constraints on the finite element model are clamped and this leads to an increase in the maximum force predicted by the finite element method.

*C. Finite element results versus corrected Amdahl and yang and Caldwell method*

Kerkegard [18] solved the problem of Yang and Amdahl methods and made some modification to that.

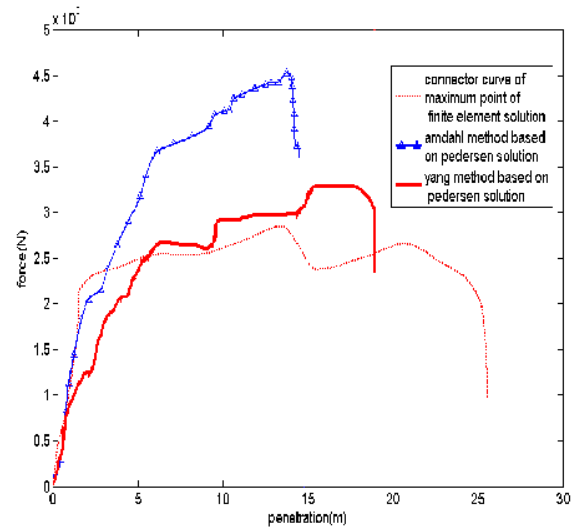


Fig. 12 comparison of the derived force-penetration curves based on the finite element and corrected yang and Amdahl's methods by Pedersen- speed=12(strain rate is considered for all methods)

Therefore, at this stage a comparison between Yang and Amdahl's corrected methods, and the finite element model is made as shown in Fig. 12. The results indicate that the predicted results by the finite element method are in complete agreement with the analytical results.

VIII. PARAMETRIC STUDY

*A. Effect of contact friction*

When two bodies collide, friction can be an effective parameter on the energy absorption and the prediction of the damage results. In this section, the effect of friction is investigated on the damage and energy dissipation. It should be pointed out that in velocities that a huge ship such as a container moves in sea, the friction coefficient of dynamic and static situations are equal. From Fig. 13, it is shown that in case of friction, part of kinetic energy is dissipated and the resultant penetration is less than the case where there is no friction. Penetration in case without friction is 8% more than the case with friction. Furthermore, a comparison between energy graphs for two cases is plotted in Fig 14.

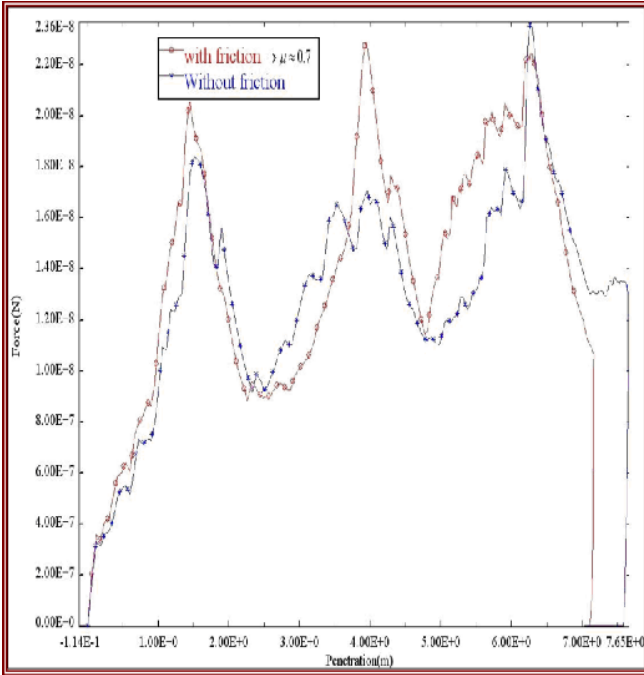


Fig. 13 Investigation of the friction effect on the resultant penetration

Figure 16 show that the strain rate affects the results. However, the effect is not very high.

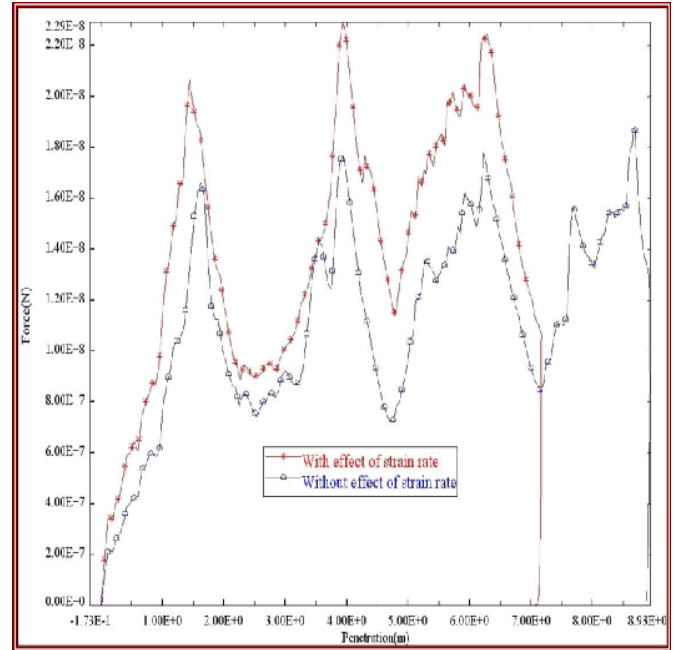


Fig. 15 Effect of strain rate on resultant penetration

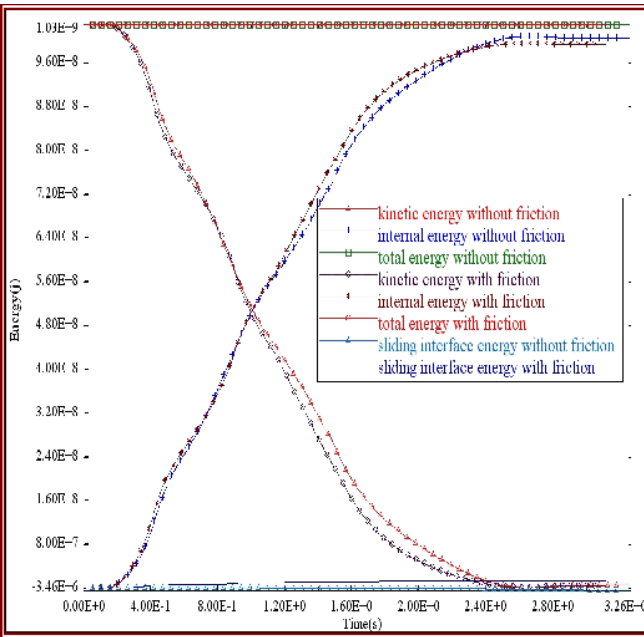


Fig. 14 investigation of energy curves in two situations (with and without effect of friction)

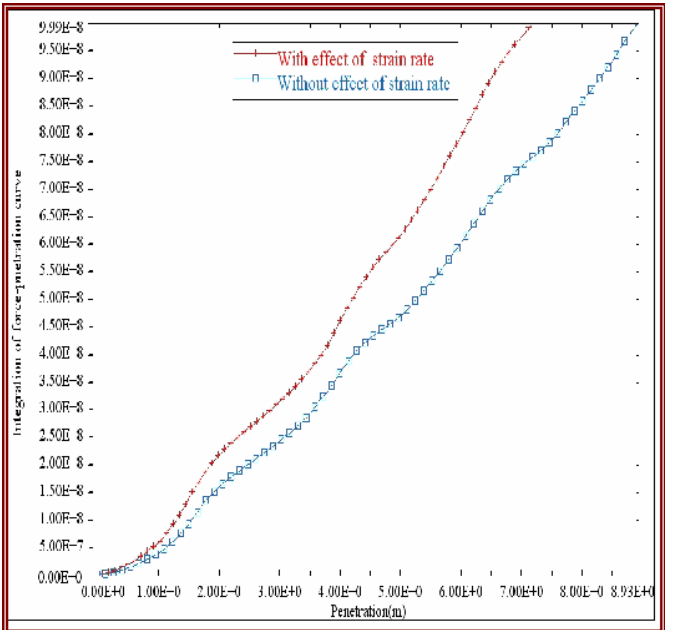


Fig. 16 Plastic deformation work in two situation (with effect of strain rate and vice versa)

### B. Effect of strain rate

Since speed of applying load on a structure increases the yield stress, this may increase the amount of final damage. Effect of this parameter has also investigated on the penetration and plastic deformation energy section (integration of force-penetration curve).

Penetration is less for the situation when the strain rate is considered (Fig. 15). The area under the force-penetration curve (force-displacement) is plastic deformation energy.

### C. Effect of ship speed on the force-penetration curve- and effect of collision angle on energy curves

In this section, the effect of the ship speed on the force-penetration curve is investigated. As shown in Figure 17, there is not a large difference between results for various speeds.

Increase in higher values of curve for the higher ship speeds is due to the effect of speed on yield stress.

In oblique collision, friction dissipation energy increases (Fig. 18). This is due to the larger contact area and larger

contact slipping speed in tangential direction. Decreasion of the linear momentum in perpendicular direction to the barrier surface causes larger contact area and larger tangential speed that leads into an increase of the friction dissipation energy.

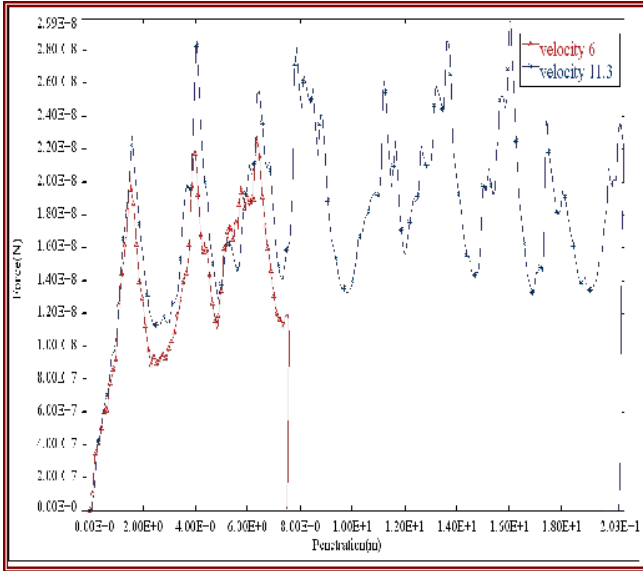


Fig.17 Effects of velocity value on forcepenetration curves

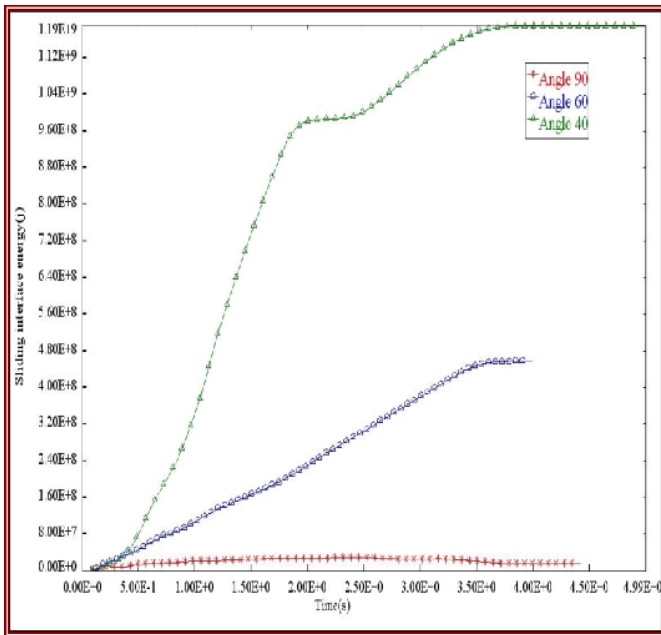


Fig. 18 Effect of collision angle on friction dissipation energy

The internal energy curve is also investigated and shown in Fig. 19. As can be seen from the figure larger values happen at angles 90, 60, and 40, respectively. As a result, by approaching the collision angle to 90, the plastic deformation energy increases.

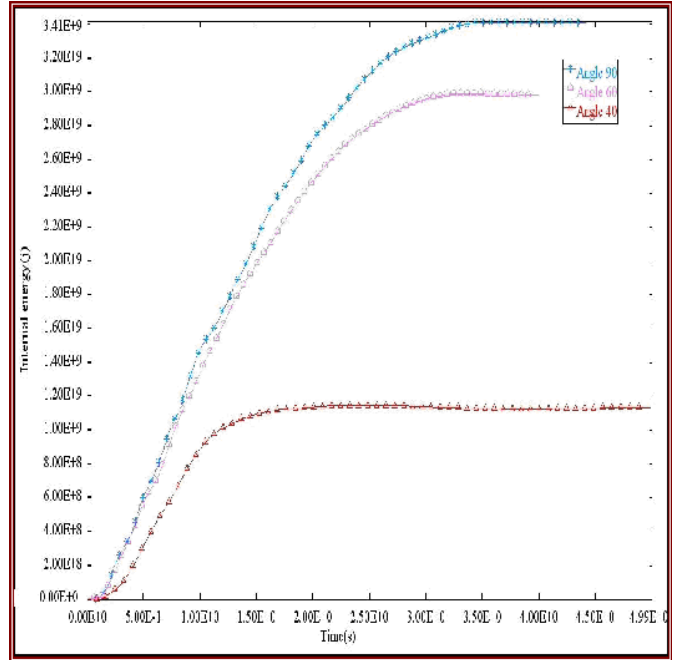


Fig. 19 Effect of collision angle on internal energy

For a better explanation, kinetic energy curves in three angles are shown in Fig. 20.

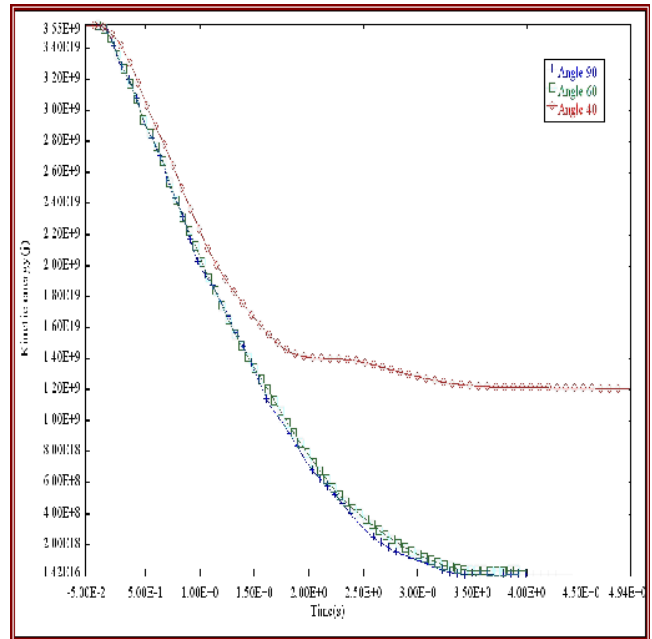


Fig. 20 Effect of collision angle on kinetic energy curves

The amount of kinetic energy for angle 40 at  $t=4s$  is due to the angular velocity of the ship. The variation of angular velocity during the contact of the ship with barrier is shown in Fig. 21. This angular velocity is not calculated directly using Ansys/Ls-Dyna. By subtracting velocity values of two points belonging to the ship along the y axis as is shown in Figures 22 and 23 and dividing the results by the distance between them, the angular velocity-time curve can be estimated.

Velocity in different directions for two considered points is shown in Fig. 22.

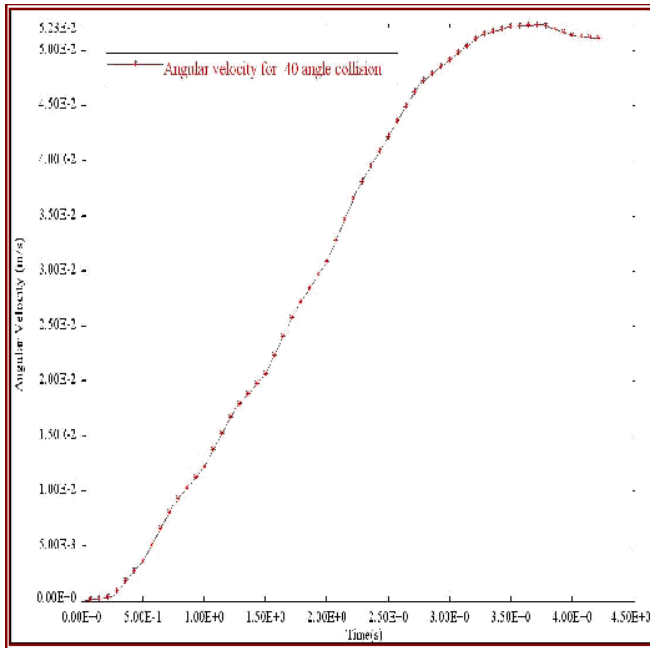


Fig. 21 Angular velocity-time curve of container ship at angle=40

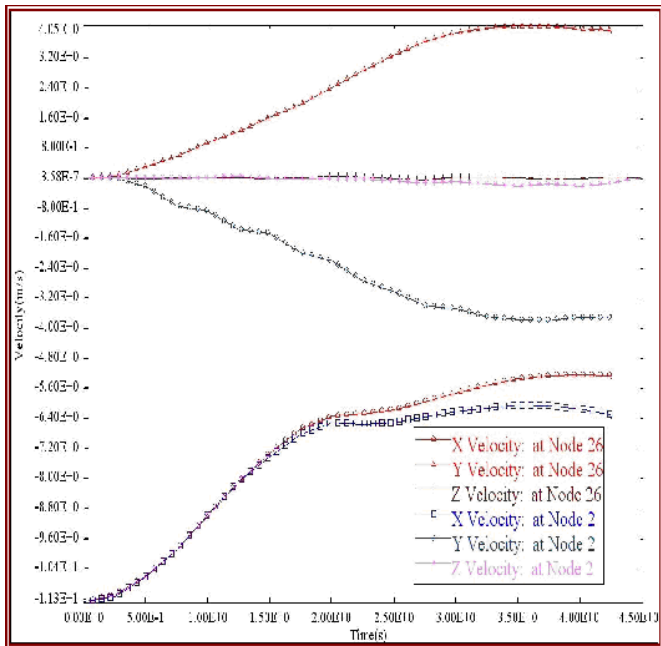


Fig. 22 Linear velocity in different directions for two considered points of the ship

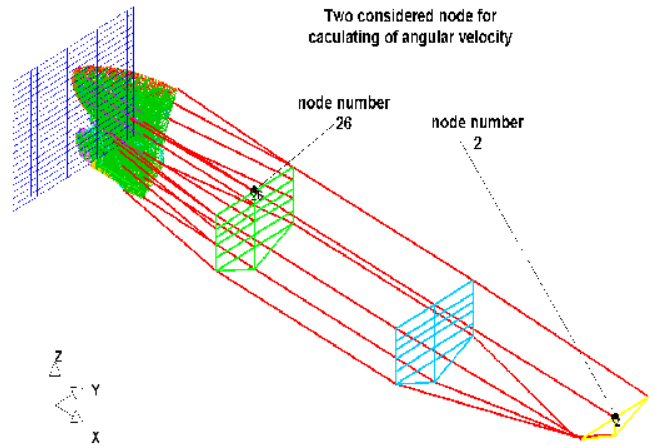


Fig. 23 Considered points belonging to the ship for determination of the angular velocity

IX. CONCLUSIONS

- 1) Variations on the values of the force-penetration curve are due to the plastic hinge lines. The maximum force occurs about the middle of the distance of the transverse frame wherever the total section reaches the yield stress and the structure collapses.
- 2) Friction can decrease penetration from 5 to 0 percent. When the collision angle approaches to 90, the effect of friction is lower.
- 3) The higher velocity increases the penetration value.
- 4) Strain rate is an effective parameter on yield stress and reduction of penetration.
- 5) Strain rate for different velocities do not affect force-penetration curve to a large extent and the results are approximately equal.
- 6) It is concluded that at the end of the collision with angle 40, ship has some kinetic energy (linear and angular). At two angles 90 and 60 the kinetic energy dissipates to the plastic and friction energy, totally. Most of the kinetic energy is dissipated to friction at angle 60 while at angle 90, the larger part of the dissipated energy is due to the plastic deformation.

REFERENCES

- [1] Minorsky, V.V. 1959, " An Analysis of Ship Collisions with Reference to Protection of NuclearPower Plants ". *Journal of Ship Research*.
- [2] McDermott J.F, Kline R.G, Jones, E.L, Maniar N.M, Chiang W.P. Tanker, 1974, "Structural Analysis for Minor Collisions", *SNAME Transaction*, Vol. 82, pp. 382-414.
- [3] Reardon P, Sprung J.L. "Validation of Minorsky's Ship Collision Model and Use of the Model to Estimate the Probability of Damaging a Radioactive Material Transportation".
- [4] Vaughan H. 1978, "Bending and Tearing of plate with Application to Ship-Bottom Damage ". *Naval Architects*. Vol. 3. pp. 97-99.
- [5] Woison G. 1979, "Design against Collision". Schiff & Hafen. Germany, Vol. 31. No. 2. pp. 1059-1069.
- [6] Paik J. K. Pedersen P.T. 1995, "Ultimate and Crushing Strength of plated Structure ". *J. of Ship Research*. Vol. 38. No. 4. pp. 340-348.
- [7] Sano A. Muragishi O. yoshikawa T. , August 22-23 , 1996, "Strength Analysis of a New Double Hull Structure for VLCC in collision". *International Conference on Design and Methodologies for Collision and Grounding Protection of Ships*. San Francisco, California, USA.

- [8] Kuroiwa T. , August 22-23, 1996, "Numerical simulation of actual collision & grounding accidents". *International conference on design and methodologies for collision and grounding protection of ships*. San Francisco, California, USA.
- [9] Kitamura O. 1997, "Comparative study on collision resistance of side structure". international conference on design and methodologies for collision and grounding protection of ships". San Francisco, California, USA, August 22-23, 1996. Also in "Marine technology", Vol. 34, No.4, pp. 293-308.
- [10] Amdahl J. and Kavlie D. 1992, "Experimental and Numerical Simulation of Double Hull stranding". *DNV-MIT Work shop on mechanics of ship collision and grounding*, DNV, Norway.
- [11] Lemmen P. M. Vredevelde W. pinkster J. A. , August 22-23.1996, "Design analysis for grounding experiments". *International conference on design and methodologies for collision and grounding protection of ships*, San Francisco, California, USA.
- [12] Lehman E. and Yu X. 1998, "Inner Dynamics of bow Collision to bridge piers". *International symposium advances in bridge aerodynamics-ship collisions analysis-operation and Maintenance*, Lyngby, Denmark.
- [13] Qvist S. Nielsen K. B. Schmidt M. H. and Madsen S. H. 1995, "Ship collision- Experimental and numerical analysis of double hull models". *9<sup>th</sup> DYMAT Technical conference*.
- [14] . McDermott J.F. Kline R.G. Jones E.L. Maniar N.M. Chiang W.P. 1974, "Tanker Structural Analysis for Minor Collisions". *SNAME Transactions*, Vol. 82, pp. 382-414.
- [15] Reckling K.A. 1983, "Mechanics of Minor Ship Collisions. *International Journal of Impact Engineering* ". Vol. 1, No. 3, pp. 281-299.
- [16] J. Amdahl. 1983, "Energy Absorption in Ship-Platform Impacts". Dr. Ing. Thesis, Report No. UR-83-84, The SS Norwegian Institute of Technology, Trondheim.
- [17] P. D. C. Yang J. B. Caldwell. 1988, "Collision energy absorption of ships bow structures". *Int. J. Impact Eng* 9 7(2).
- [18] H. Kierkegaard. 1993, "Ship bow response in high energy collision". To be published in *Marine Structures*. Vol6, pp. 359-356.
- [19] Hysing T. 1995, "Damage and penetration analysis-safety of passenger/RoRo vessels", DNV Report No. 95-0419, Norway.
- [20] Scharrer M. Ostergaard C. 1996, "Safety of Passenger/RoRo Vessels- Analysis of collision energies and Hole sizes ". Germanischer Lloyd, Report No.FL96.009, Hamburg.
- [21] Wang G. Ohtsubo H. 1997, "Deformation of ship plate subjected to very large load ". OMAE.
- [22] Wierzbicki T. , 1983, "Crushing Behavior of Plate Intersections". *Structural Crashworthiness*. edited by A Jones T Wierzbicki. Chapter 3, Butterworth and Co., London.
- [23] Pedersen P.T., et al. 1993, "Ship Impacts: Bow Collisions." *International Journal of Impact Engineering*. Vol. 13, No. 2, pp. 163-187.
- [24] Brown A.J. 2002, "Modeling Structural Damage in Ship Collision". SSSC Collision Report.
- [25] Xia. Jianjun. 2001, "Finite Element Analysis of Ship Collisions". Master of science thesis in ocean engineering .
- [26] G. Gerard. 1958. "The crippling strength of compression elements". *J. Aeronaut. Sci.*
- [27] N Jones. 1983. "Structural aspects of ship collisions". In *Structural Crashworthiness*, Edited by Jones N Wierzbicki T. pp. 308-337. Butterworths, London.
- [28] Saul R. Svensson H. 1983. "Means of reducing consequences of ship collisions with bridges and offshore structures". I ABSE Colloquium on Ship Collision with Bridges and Offshore Structures, Copenhagen.